Colorimetric determination of *p*-nitrophenol on ELISA microwells modified with an adhesive polydopamine nanofilm containing catalytically active gold nanoparticles

Simona Scarano*, Pasquale Palladino, Emanuela Pascale, Alvaro Brittoli, and Maria Minunni

Department of Chemistry 'Ugo Schiff', University of Florence, Via della Lastruccia 3-13, 50019, Sesto Fiorentino, Italy

*e-mail: simona.scarano@unifi.it

Abstract

A microplate method is described for the quantification of *p*-nitrophenol (*p*-NPh) in urine samples where it can be found after exposure to certain insecticides such as methyl parathion or paraoxon. The assay is based on the use of a polydopamine (PDA) film doped with gold nanoparticles (AuNPs). The latter exerts a catalytic effect on the reduction of nitrophenols by $NaBH_4$. PDA has adhesive properties and can be used to fix the AuNPs on several solid substrates, here ELISA polystyrene microwells. The optical and catalytic properties of different populations of AuNPs spontaneously grown on PDA films were investigated, mainly in terms of the relationship between AuNPs@PDA nanocomposite preparation and its catalytic activity and stability. The reduction of *o*-, *m*-, and *p*-nitrophenols by $NaBH_4$ in aqueous solution was exploited as model study. The approach demonstrates that useful kinetic information on the catalytic effect can be obtained on 96-wells simultaneously by a conventional ELISA reader at a fixed wavelength of 415 nm. The method was successfully applied to the quantification of *p*-NPh in (spiked) urine samples and gave high reproducibility (RSD = 3.5%) and a 6.30 µM (836 µg/L) detection limit.

Keywords: nanocomposite materials, urine analysis, metallic nanostructures, (bio)polymers, redox catalysts, organic reactions, high-throughput screening, UV-vis spectroscopy, plasmons, cathecols

Introduction

The use of nanocomposite materials represents an emerging and very useful possibility to develop cheap, user friendly, and disposable analytical platforms for simple results reading and easy access for a variety

of analytical problems. In this context, polymeric/metallic nanostructures-based nanocomposites may play an extremely interesting role. Gold nanostructures have been widely employed in bioanalytical approaches with different strategic roles [1], and now can be widely found integrated with (bio)polymers to investigate new and original features with perspective applications in different fields [2]. Among others, in a wider spectrum of applications, gold nanoparticles (AuNPs) are extensively used as efficient and size-dependent redox catalysts [3]. In particular, the preparation of supported AuNPs for the catalysis of organic reactions is mainly realized by the use of inorganic species such as metal oxides, active carbon, and silica spheres. As alternative, organic polymers [4,5] and magnetic nanoparticles [6,7] represent popular commercialized options. In this framework, polydopamine (PDA) has been introduced for the effective coating of magnetic microspheres and nanotubes [8-10]. This intriguing self-assembling and adhesive polymer is able to form stable nanometric films on almost any surface [11] and has displayed to be an extremely efficient and convenient alternative support for metallic nanocatalysts, mainly gold [12]. Moreover, due to the reduction potential of cathecols of PDA (E°=-0.699 V *vs* normal hydrogen electrode, NHE), Au(III) can be efficiently reduced to Au(0) (E°=0.994 V *vs* NHE) at the polymer surface, thus allowing gold nanoparticles to grow *in situ* on any support without using any reducing agent or metallic seed particles. The nanocomposite is here named AuNPs@PDA and, to our best knowledge, is here reported for the first time as catalytically active substrate for analytical purposes. In particular, here it is realized a new and original way to modify ELISA microwell with AuNPs@PDA in a reproducible and high-throughput manner for *p*-nitrophenol quantification in urine through its heterogeneous catalytic reduction. The reactions were conveniently monitored by UV-vis spectroscopy [13] by an ELISA reader at fixed wavelength on 96-wells simultaneously. The catalytic activity of different populations of AuNPs grown on PDA was investigated and rationalized for the model reduction in water of all the three NPh isomers (*orto*, *meta*, and *para* NPh) to aminophenols (APh), in presence of NaBH$_4$. This approach allowed to identify the best preparation conditions of the catalytic substrate, and to infer important and original considerations on AuNPs@PDA. Interestingly, it is observed a strict relation between the metal ion precursor Au(III) concentration ([Au]) and the chemical resistance of the final nanocomposite during the catalytic reduction. Therefore, this parameter was extensively investigated to obtain a stable nanocomposite useful for our purposes. Moreover, it is evident that the plasmon signal elicited by gold nanoparticles on the microwell can be conveniently monitored to assess the destiny of the nanocatalyst during the process, and this represents an inspiring result also useful in catalysis research fields based on the use of supported gold nanoparticles. The optimized protocol was exploited to set up an original, high throughput *in-plate* method to quantify nitrophenols in aqueous

solution, determining the main kinetic and analytical parameters. Finally, results on standard samples were directly compared with those obtained on spiked urine samples containing *p*-NPh, the main bodily fluid of interest for its monitoring [14-18].

2. Experimental

2.1 Reagents, materials, and instrumentation

Dopamine hydrochloride (DA), hydrogen tetrachloroaurate trihydrate (HAuCl$_4$•3H$_2$O, >99.0%), Trizma hydrochloride (Tris-HCl, >99.0%), sodium borohydride (NaBH$_4$), *o*-nitrophenol, *m*-nitrophenol, *p*-nitrophenol, and *o*-aminophenol were all purchased from Sigma-Aldrich (Milan, Italy, www.sigmaaldrich.com/italy). All chemicals were used as received without any further purification. Milli-Q water with a resistivity of 18.2 MΩ cm was used in preparation of all the solutions (Merck Millipore, Italy, http://www.merckmillipore.com/IT/it) and all experiments were carried out at room temperature. Disposable polystyrene ELISA microwell working on iMark™ Microplate Absorbance Reader (Bio-Rad, Milan, Italy, http://www.bio-rad.com), were supplied by Sarstedt (Milan, Italy, https://www.sarstedt.com). UV-Vis absorption spectra were recorded with an OceanOptics spectrometer (https://oceanoptics.com) including a tungsten halogen light source for the Vis-NIR (HL-2000-FHSA), a customized fiber optic probe working in reflectance, and a miniature spectrometer (Flame-T).

2.2 Au@PDA ELISA-type microwells preparation

PDA films were prepared from fresh solutions of dopamine hydrochloride, 5 mg/mL in 10 mM Tris–HCl buffer, pH 8.5. ELISA microwells (96) were quickly filled with 100 μL of DA solution and PDA polymerization was performed for 24 h in static conditions at room temperature. Therefore, wells were emptied, rinsed with deionized water, and dried under filtered air flow. Successively, 100 μL of aqueous solution of HAuCl$_4$•3H$_2$O at different concentrations was added to each PDA-coated well and lasted for 24 h in the dark at room temperature. The plates were finally rinsed with Milli-Q water, dried with air, and kept sealed in the dark until further use.

2.3 Characterization of PDA and AuNPs growth on microwell

The UV-vis absorption spectra of fabricated samples were recorded by using a Shimadzu 2600 UV–vis–near-IR spectrophotometer (www.shimadzu.com). The scanning electron microscopy (SEM) experiments were carried out by using a Zeiss NVISION 40 dual beam Focused Ion Beam (FIB) system, equipped with a high-resolution SEM Gemini column (www.zeiss.com). The morphological analyses were performed under suitably selected observation conditions, in order to limit the charging effects due to the highly insulating nature of the substrate. In particular, a beam current of 5 pA and an accelerating voltage of 500 V were used to investigate the samples. Secondary electron (SE) images were acquired by using the Everhart Thornley SE detector.

2.4 Nitrophenol isomers reduction on Au@PDA coated microwell

Microwell plates coated with AuNPs@PDA were filled with 100 µL of NPh aqueous solutions and their catalytic reduction was followed through the decrease of absorbance intensity of nitrophenolate ion (@415 nm) up to 1 h, with 1 min interval time on the ELISA reader. To homogeneously compare the catalytic performance of different AuNPs@PDA coatings grown onto the plates, all the NPh solutions tested contained, separately, 100 µM (13.9 mg/L) of each NPh and 0.1 M of $NaBH_4$. As negative controls, the same NPh solutions without $NaBH_4$, and $NaBH_4$ alone were also tested following the same procedure. Microwells coated only with PDA, excluding AuNPs growth, were also subjected to investigation to evaluate possible reducing activity of PDA itself. For NPhs calibration, once selected the most efficient preparation protocol for AuNPs@PDA coatings, each NPh isomer was calibrated within the concentration range 10-500 µM. Molar extinction coefficients (ε) for NPhs were calculated by calibrating each NPh isomer in the experimental conditions used for their catalytic reduction at t=0, and plotting absorbance values against concentration.

2.5 Urine samples analysis

Urine samples collected from volunteers were spiked with *p*-NPh at different final concentrations ranging from 1.00 mM to 10.0 µM (139 to 1.39 mg/L). Spiked and unspiked urine samples were subjected to the same steps except for *p*-NPh addition. *p*-NPh positive and negative urine samples were promptly heated at 95 °C for 10 min, centrifuged at 14000 rcf for 10 min, and then filtered on 0.22 µm filters. Urine samples were then transferred in microwells and added with $NaBH_4$ by following the previous reaction protocol reported in water. The reduction reaction was followed at 415 nm for 300 sec. In the same microwell plate carrying urine samples, at least three columns (3x8=24 wells) were used for *p*-NPh

calibration in distilled water, and data from calibrator and real samples were collected at the same time.

3. Results and discussion

3.1 Optimization of AuNPs@PDA substrates for NPhs reduction

One of the main attractive features of AuNPs@PDA substrates is the possibility to modulate their final characteristics by changing the system variables. Dopamine concentration, pH, growth time, supporting material, and metal precursor concentration/incubation time are all interesting and valuables parameters that may be considered, singularly or in combination. In a previous work [19], it has been reported the effect of PDA thickness on the plasmonic features of the AuNPs subsequently grown on its surface, showing a linear correlation between PDA thickness and its reducing power toward Au(III), also showing the relation between PDA thickness and different AuNPs plasmonic behaviors obtainable. Since the state of art lacks information regarding the role of different AuNPs populations on the polymer surface in terms of catalytic activity, here it has been rationally investigated this aspect and exploited for analytical purposes. Substrates obtained by using 0.5 mM Au(III) for the *in-situ* growth of AuNPs@PDA surface displayed excellent behaviors for the all three NPhs isomers in terms of resistance and substrate conversion (see electronic supplementary materials). Therefore, this concentration has been used for kinetics experiments.

3.2 Reduction kinetics of NPhs isomers on AuNPs@PDA in standard conditions

The three isomers were serially tested in real time on ELISA microwell to deeper investigate kinetic trends of reactions. Through the proposed approach, a useful double check of the reaction course can be also easily obtained, by monitoring at the same time the substrate reduction and the behavior of the catalyst over time by classical spectrophotometry, as reported in Fig. 1. While the absorbance of NPh decreases, possible change related to AuNPs may be evidenced by the observation of the plasmon band. Its position and intensity in water before (black line) and during the reaction attests the optimal persistence of AuNPs. This approach results innovative respect to the current literature in the field and consists in the great advantage to check the persistence of the composite nanomaterial in case of different catalytic reactions.
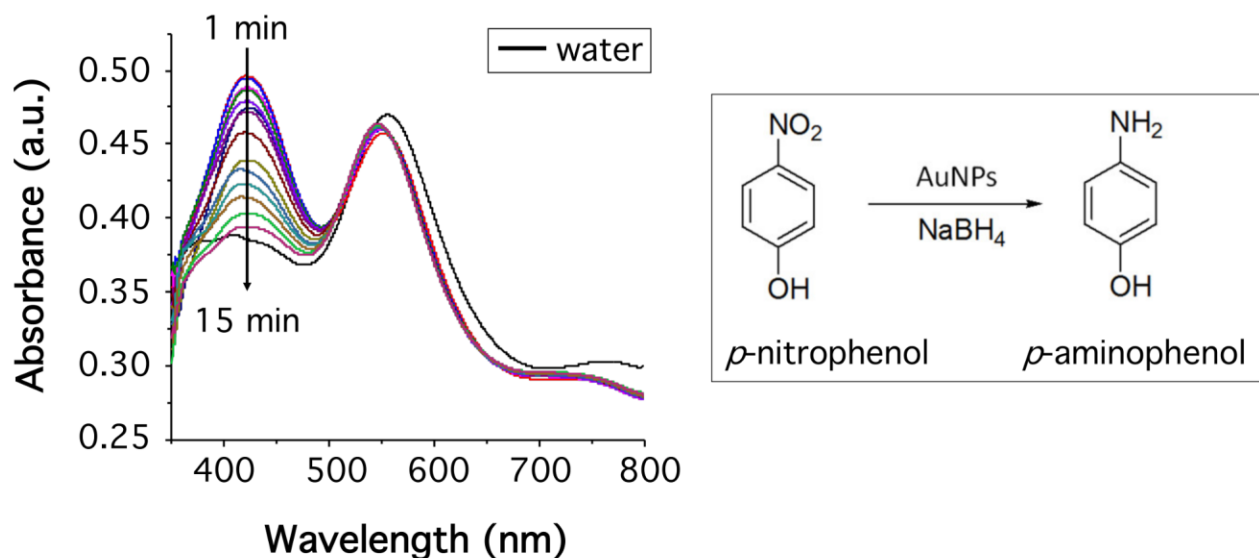
Fig. 1. Catalytic reduction of *p*-NPh (100 µM; 13.9 mg/L) by AuNPs@PDA monitored by classical spectrophotometry. At about 415 nm the decrease of the *p*-nitrophenolate ion is evidenced by the arrow. The AuNPs population grown on the PDA layer is responsible for the plasmon band at about 550 nm that is clearly distinguishable from the *p*-NPh signal.

Using a large excess of NaBH$_4$ (0.1 M) compared to [NPh], a pseudo-first order reaction kinetic may be applied for evaluating the catalytic rates of the three isomers. As expected, the observed rate constants (k, min^{-1}×10^{-3}) resulted significantly different among isomers and, as reported in Fig. 2a, *m*-NPh displays the worst performance both in terms of rate conversion and optical features. In Fig. 2b the supposed mechanism for NPh catalytic reduction by means of AuNPs@PDA is sketched. As reported for similar supported nanocatalysts based on AuNPs [20], it involves the transfer of hydrogen species from BH$_4^-$ to AuNPs surface, which allows the subsequent reduction of NPh to aminophenol (APh).
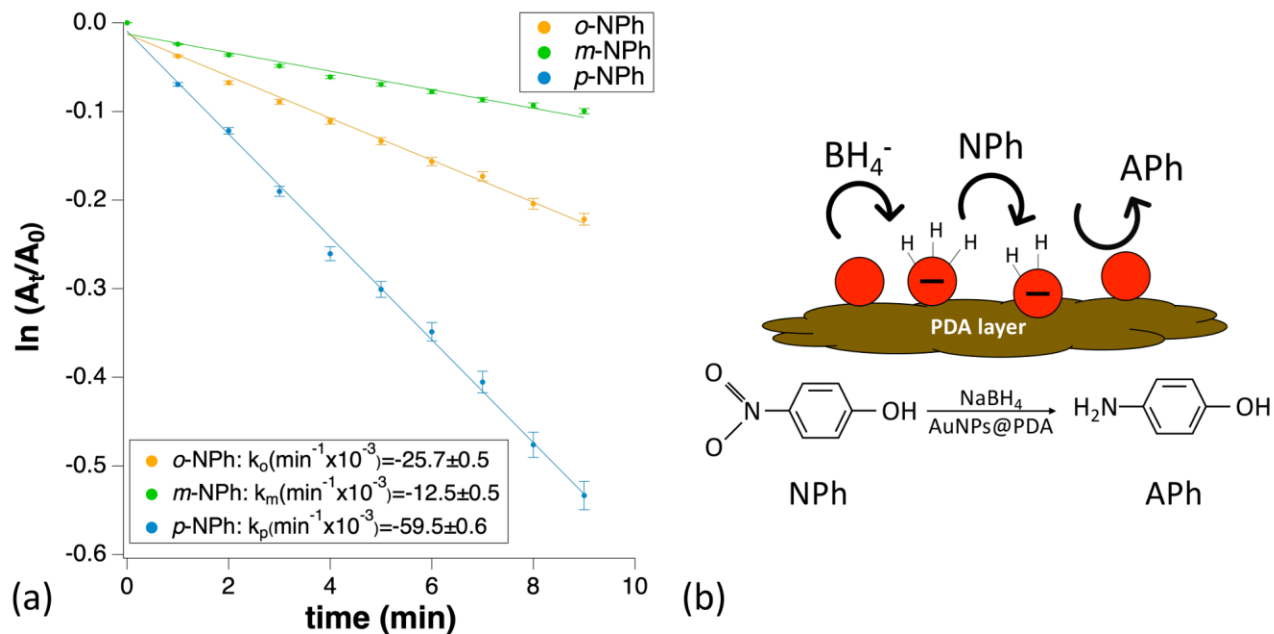
Fig. 2. (a) Linear correlation of ln(A_t/A_0) vs time (min) for the three NPhs isomers tested, and the relative rate constants calculated from the slopes. (b) Representation of the hypothesized reduction mechanism of NPhs in presence of AuNPs@PDA.

3.3 Quantification of *p*-nitrophenol in water and urine on AuNPs@PDA substrate

To quantitatively exploit the optimized catalytically active nanocomposite, it has been investigated the possibility of testing *o*-, *m*-, and *p*-NPh both in water and in human urine. In fact nitrophenols, especially *o*- and *p*-NP, are well-known environmental pollutants with important impact on human and animal health. They are the degradation products of pesticides and fungicides, mainly methyl parathion and paraoxon [21], cars and industrial wastes, and lignin and humic acid present in soil. In particular, the analytical determination of *p*-nitrophenol is of outmost importance for several purposes, *i.e.* environmental screening, epidemiological studies, toxicological assays etc. To date, the quantitative determination of this compound generally remains the prerogative of classical techniques like HPLC or expensive ones like HPLC-MS with the use of radiolabels. As less expensive and portable alternative, electrochemical sensing methods have been also reported, based on the oxidative determination of *p*-nitrophenol on glassy, platinum, and gold electrodes modified following different strategies [22-25]. In this framework, it has been investigated the possible use of this approach as alternative to the existent methods.

The dose response effect was first tested in standard conditions, *i.e.* NPhs diluted in distilled water in the range 10.0-500 μM (1.39-69.6 mg/L) for the three isomers (Fig. 3a). As already inferred from kinetic

7

data, *p*-NPh shows the most sensitive response to concentration changes, with the highest molar extinction coefficient (ε) under the investigated conditions, *i.e.* ε(*p*-NPh)=3245 M^{-1} cm^{-1}, compared to ε(*o*-NPh)=1169 M^{-1} cm^{-1} and ε(*m*-NPh)=366 M^{-1} cm^{-1}. Despite all the isomers show high linearity, *m*- and *o*-NPh result scarcely usable for quantitative purposes due to low slope and ε values. On the contrary, *p*-NPh displays optimal features that may be exploitable for its detection in real samples. The averaged relative standard variation (RSD) within the whole calibration range is 3.5% (n=3), which allows to calculate a limit of detection (LOD) in distilled water for *p*-NPh of 6.30±0.01 μM (836±1 μg/L) (LOD = 3σ/m; where σ is the standard deviation of the blank and m is the slope of the calibration plot). This result is in line respect to several electrochemical methods for water analysis, but these latter are not suitable for high throughput screening, permitted by the here presented method (up to 96 independent results in 2 minutes); moreover, here is not required any complex and tedious preparation of electrode surfaces and delicate pre-concentration steps [26-28].

This result encouraged us to move forward by testing the effectiveness of the protocol in real matrices. In this framework, on the base of the current literature, it has been selected human urine as reference specimen bodily fluid for *p*-NPh quantification [14,29-31]. To this aim, the same protocol adopted for aqueous solutions was applied to real samples, introducing a simple thermal pretreatment followed by filtration before the assay. Urine samples were tested with and without *p*-NPh spikes at the same concentration points used in standard conditions, i.e. distilled water, and results were directly compared (Table 1 and Fig. 3b).

Table 1
Recovery data at different concentrations of *p*-NPh in urine samples. Standard deviations (SD) are calculated on n=5 independent replicates on the same microwell plate.

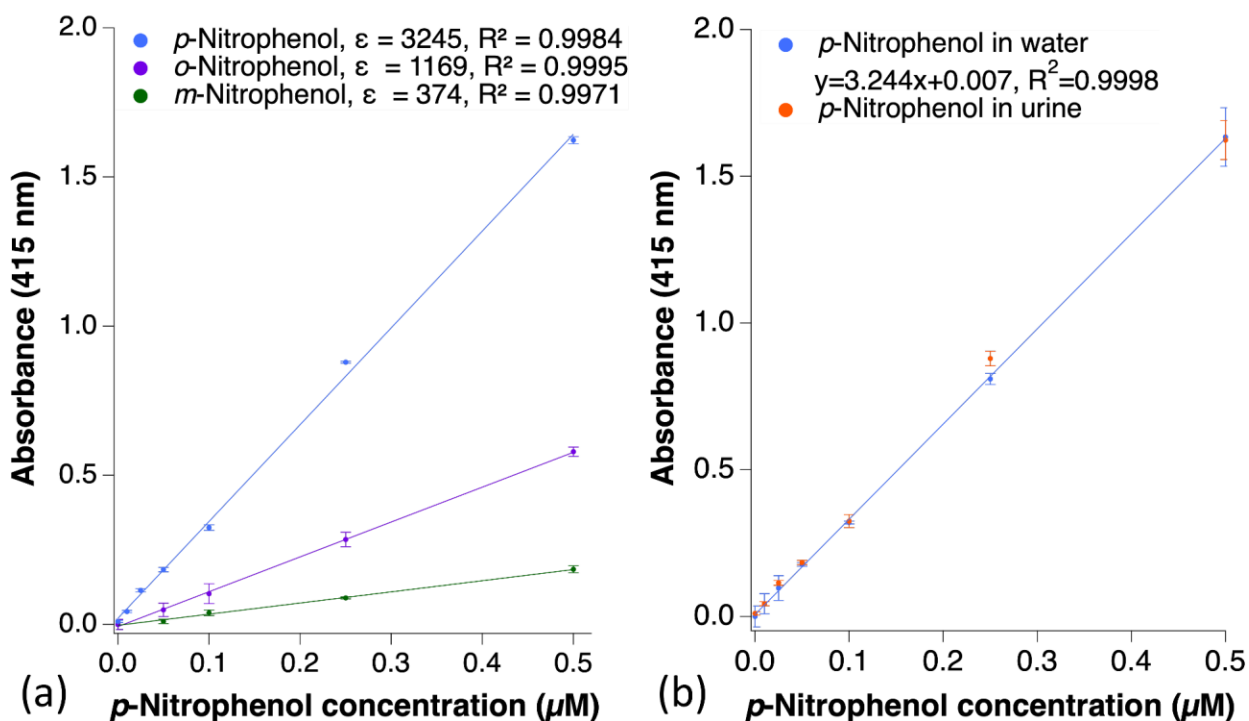| Spiked *p*-NPh (μM)	Absorbance±SD in urine (a.u.)	Absorbance±SD in water (a.u.)	Recovery in urine (%)
0.500	1.623±0.066	1.634±0.100	99.3
0.250	0.879±0.025	0.809±0.019	108.6
0.100	0.325±0.022	0.320±0.005	101.5
0.050	0.184±0.007	0.177±0.006	103.6
0.025	0.114±0.008	0.097±0.042	118.3
0.010	0.043±0.007	0.043±0.034	100.0
0.000	0.010±0.008	0.010±0.036	100.0

Fig. 3. (a) Linear calibration of *o*-, *m*-, and *p*-nitrophenols in distilled water. Absorbance values are taken at 120 s and 415 nm; standard deviations are calculated on three independent replicates. (b) Direct comparison of the dose response in distilled water and in human urine spiked with the same *p*-NPh concentration points used for the calibration. Standard deviations are calculated on five independent replicates on the same microwell plate.

Data reported in the plot are relative to absorbance at 415 nm after 120 s of reaction, and standard deviations are inferred both for calibrator and real samples from five independent replicates on the same ELISA plate. As clearly evidenced by the overlapping of the linear trends, the quantification of *p*-NPh in urine does not show any negative effect due to the real matrix. Obviously, due to the natural color of urine, as expected, a background absorbance at 415 nm is recorded for all the samples. However, this effect is here corrected by the simple subtraction of the absorbance of unspiked urine from all the measurements. As reported in the plot of Fig. 3b, the subtraction sets to zero-absorbance the unspiked urine and allows the correct quantification of all the other samples. Moreover, it is noteworthy that unspiked urine added with NaBH$_4$ and tested in AuNPs@PDA modified ELISA microwells does not show any reactivity, giving no absorbance change over time. Recovery has been calculated and reported in Table 1 for all the urine spiked samples by comparison with the calibration curve of *p*-NPh in distilled

water. The RSD averaged on five independent calibrations and all the concentration points (n=6) resulted 6.8%, a very good result, with negligible difference in the limit of detection between distilled water and urine samples. As expected, the micromolar detection limit here showed in urine (6.30 μM; 836 μg/L) results far from more sensitive but time and cost expensive analytical platforms, *e.g.* 37 nM (5.2 μg/L) by HPLC-MS/MS, [30] representing the major limitation of the procedure. However, it is close to the low-micromolar limit (2-4 μM; 300-600 μg/L) established by the US Environmental Protection Agency and the European Commission, for urine positiveness in adult (≥16 years) making the method suitable for classifying samples into the various priority levels required for public health intervention [31].

Conclusions

The development of new and performing analytical methods cannot ignore the need to evaluate original uses of conventional analytical instrumentation, widely present in control laboratories. Here it is demonstrated how disposable microwell used for immunochemical routine ELISA assays can be successfully revisited for the quantitative determination of *p*-nitrophenol (*p*-NPh) in human specimens such urine. This result is achieved by means of the self-assembling of dopamine to form adhesive nanofilms of PDA on almost any type of surfaces, polystyrene in this case, coupled to its reducing ability towards Au (III) to form AuNPs at the surface. The resulting composite nanomaterial, here named AuNPs@PDA, was exploited as catalytically active substrate to obtain the colorimetric determination of *p*-NPh on a conventional plate reader at 415 nm, in minutes and with high reproducibility and good sensitivity.

Despite the use of AuNPs supported on PDA films has been reported before for catalysis purposes [12], the investigation here is expanded to the relationship between the nanocomposite preparation and its catalytic activity. The study, as well as being interesting in itself, proves here to be further extended to original and quantitative analytical purposes.

The results reinforce the whole strategy presented and let foresee the development of further promising applications on this platform. In fact, similar results may be obtained for the catalytic reduction of other molecules of interest in different fields. The convenient position of the absorbance band of AuNPs@PDA and that of the putative analyte should be carefully evaluated as pre-requisite. However, the use of different metal precursors for PDA decoration with NPs, and/or specific final NPs shapes would give the chance to shift the plasmon band along the wavelength window, to avoid absorbance overlapping. This

approach represents a fast, low cost, and reproducible assay suitable for fast screening, alternative to classical and new methods.

Electronic supplementary material. The online version of this article contains supplementary material, which is available to authorized users.

Corresponding Author

*simona.scarano@unifi.it. Tel.: +39 0554573283

ORCID

Simona Scarano: 0000-0002-8050-1715

Compliance with ethical standards The authors declare that they have no competing interests.

References

[1] Tokonami S, Yamamoto Y, Shiigi H, Nagaoka T (2012) Synthesis and bioanalytical applications of specific-shaped metallic nanostructures: A review. Anal Chim Acta 716:76-91. https://doi.org/10.1016/j.aca.2011.12.025

[2] Ofir Y, Samanta B, Rotello VM (2008) Polymer and biopolymer mediated self-assembly of gold nanoparticles. Chem Soc Rev 37:1814-1825. https://doi.org/10.1039/B712689C

[3] Alshammari A, Kalevaru VN (2016) Supported gold nanoparticles as promising catalysts. In catalytic application of nano-gold catalysts. InTech Open. https://doi.org/10.5772/64394

[4] Linares N, Silvestre-Albero AM, Serrano E, Silvestre-Albero J, Garcia-Martinez J (2014) Mesoporous materials for clean energy technologies. Chem Soc Rev 43:7681–7717. https://doi.org/10.1039/C3CS60435G

[5] Tang J, Shi Z, Berry RM, Tam KC (2015) Mussel-inspired green metallization of silver nanoparticles on cellulose nanocrystals and their enhanced catalytic reduction of 4-nitrophenol in the presence of b-cyclodextrin. Ind Eng Chem Res 54:3299–3308. https://doi.org/10.1021/acs.iecr.5b00177
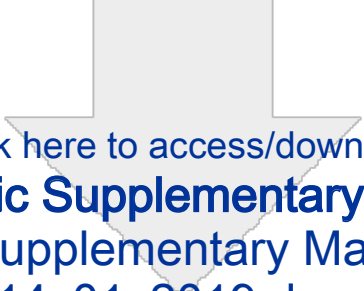
[6] Shokouhimehr M (2015) Magnetically separable and sustainable nanostructured catalysts for heterogeneous reduction of nitroaromatics. Catalysts, 5:534-560. https://doi.org/10.3390/catal5020534

[7] Yoon TJ, Lee W, Oh YS, Lee JK (2003) Magnetic nanoparticles as a catalyst vehicle for simple and easy recycling. New J Chem 27:227-229. https://doi.org/10.1039/B209391J

[8] Zeng T, Niu HY, Ma YR, Li WH, Cai YQ (2013) In situ growth of gold nanoparticles onto polydopamine-encapsulated magnetic microspheres for catalytic reduction of nitrobenzene. Appl Catal B 134:26-33. https://doi.org/10.1016/j.apcatb.2012.12.037

[9] Wei Q, Shi R, Lu D, Lei Z (2016) In situ formation of gold nanoparticles on magnetic halloysite nanotubes via polydopamine chemistry for highly effective and recyclable catalysis. RSC Adv 6:29245-29253. https://doi.org/10.1039/C6RA02789J

[10] Bakirci G, Yilmaz M, Babur E, Ozden D, Demirel G (2017) Understanding the effect of polydopamine coating on catalytic reduction reactions. Catal Commun 91:48-52. https://doi.org/10.1016/j.catcom.2016.12.018

[11] Lee H, Dellatore SM, Miller WM, Messersmith PB (2007) Mussel-inspired surface chemistry for multifunctional coatings. Science 318:426-430. https://doi.org/10.1126/science.1147241

[12] Wang JG, Hua X, Li M, Long YT (2017) Mussel-inspired polydopamine functionalized plasmonic nanocomposites for single-particle catalysis. ACS Appl Mater Interfaces 9:3016-3023. https://doi.org/10.1021/acsami.6b14689

[13] Herves P, Perez-Lorenzo M, Liz-Marzan LM, Dzubiella J, Lu Y, Ballauff M (2012) Catalysis by metallic nanoparticles in aqueous solution: model reactions. Chem Soc Rev 41:5577-5587. https://doi.org/10.1039/C2CS35029G

[14] Barr DB, Turner WE, DiPietro E, McClure PC, Baker SE, Barr JR, Gehle K, Grissom RE Jr, Bravo R, Driskell WJ, Patterson DG Jr, Hill RH Jr, Needham LL, Pirkle JL, Sampson EJ (2002) Measurement of p-nitrophenol in the urine of residents whose homes were contaminated with methyl parathion. Environ Health Perspect 110:1085–1091. https://doi.org/10.1289/ehp.02110s61085

[15] Han DH, Jung DG, Shin HS (2008) Determination of parathion metabolite, p-nitrophenol in urine of parathion factory workers. Bull Korean Chem Soc 29:985-987. https://doi.org/10.5012/bkcs.2008.29.5.985

[16] Almási A, Fischer E, Perjési P (2011) HPLC Quantification of 4-Nitrophenol and its conjugated metabolites from bile. Sci Pharm 79:837-847. https://doi.org/10.3797/scipharm.1106-22

[17] Ghazizadeh AJ, Afkhami A, Bagheri H (2018). Voltammetric determination of 4-nitrophenol using a glassy carbon electrode modified with a gold-ZnO-SiO$_2$ nanostructure. Microchim Acta, 185:296. https://doi.org/10.1007/s00604-018-2840-4

[18] Karthik P, Pandikumar A, Preeyanghaa M, Kowsalya M, Neppolian B (2017). Amino-functionalized MIL-101(Fe) metal-organic framework as a viable fluorescent probe for nitroaromatic compounds. Microchim Acta, 184:2265-2273. https://doi.org/10.1007/s00604-017-2215-2

[19] Scarano S, Pascale E, Palladino P, Fratini E, Minunni M (2018) Determination of fermentable sugars in beer wort by gold nanoparticles@polydopamine: a layer-by-layer approach for Localized Surface Plasmon Resonance measurements at fixed wavelength. Talanta 183:24-32. https://doi.org/10.1016/j.talanta.2018.02.044

[20] Eo M, Baek J, Song HD, Lee S, Yi J (2013) Quantification of electron transfer rates of different facets on single gold nanoparticles during catalytic reactions. Chem Commun 49:5204-5206. https://doi.org/10.1039/C3CC41627E

[21] Barr DB, Needham LL (2002) Analytical methods for biological monitoring of exposure to pesticides: a review. J Chromatogr B 778:15–29. https://doi.org/10.1016/S1570-0232(02)00035-1

[22] Hu S, Xu C, Wang G, Cui D (2001) Voltammetric determination of 4- nitrophenol at a sodium montmorillonite-anthraquinone chemically modified glassy carbon electrode. Talanta 54:115–123. https://doi.org/10.1016/S0039-9140(00)00658-5

[23] Lupu S, Lete C, Marin M, Totir N, Balaure PC (2009) Electrochemical sensors based on platinum electrodes modified with hybrid inorganic–organic coatings for determination of 4-nitrophenol and dopamine. Electrochim Acta 54:1932–1938. https://doi.org/10.1016/j.electacta.2008.07.051

[24] Arcinte A, Mahosenaho M, Pinteala M, Sesay A-M, Virtanen V (2011) Electrochemical oxidation p-nitrophenol using graphene-modified electrodes, and a comparison to the performance of MWNT-based electrodes. Microchim Acta 174:337–343. https://doi.org/10.1007/s00604-011-0628-x

[25] Xu G, Yang L, Zhong M, Li C, Lu X, Kan X (2013) Selective recognition and electrochemical detection of p-nitrophenol based on a macroporous imprinted polymer containing gold nanoparticles. Microchim Acta 180:15-16. https://doi.org/10.1007/s00604-013-1090-8

[26] Rawajfih Z, Nsour N (2006) Characteristics of phenol and chlorinated phenols sorption onto surfactant-modified bentonite. J Colloid Interface Sci 298:39–49. https://doi.org/10.1016/j.jcis.2005.11.063

[27] Jinadasa KBSN, Mun CH, Aziz MA, Ng WJ (2004) Acidogenic pretreatment of wastewaters containing 2-nitrophenol. Water Sci Technol 50:119-124. https://doi.org/10.2166/wst.2004.0503

[28] Musilová J, Barek J, Pecková K (2011) Determination of nitrophenols in drinking and river water by differential pulse voltammetry at boron-doped diamond film electrode. Electroanalysis 23:1236-1244. https://doi.org/10.1002/elan.201100016

[29] Hill RH Jr, Shealy DB, Head SL, Williams CC, Bailey SL, Gregg M, Baker SE, Needham LL (1995) Determination of pesticide metabolites in human urine using an isotope dilution technique and tandem mass spectrometry. J Anal Toxicol 19:323–329. https://doi.org/10.1093/jat/19.5.323

[30] Sampson EJ (2002) Measurement of p-nitrophenol in the urine of residents whose homes were contaminated with methyl parathion. Environ Health Perspect 110:1085–1091. https://doi.org/10.1289/ehp.02110s61085

[31] Hryhorczuk DO, Moomey M, Burton A, Runkle K, Chen E, Saxer T, Slightom J, Dimos J, McCann K, Barr D (2002) Urinary p-nitrophenol as a biomarker of household exposure to methyl parathion. Environ Health Perspect 110:1041-1046. https://doi.org/10.1289/ehp.02110s61041
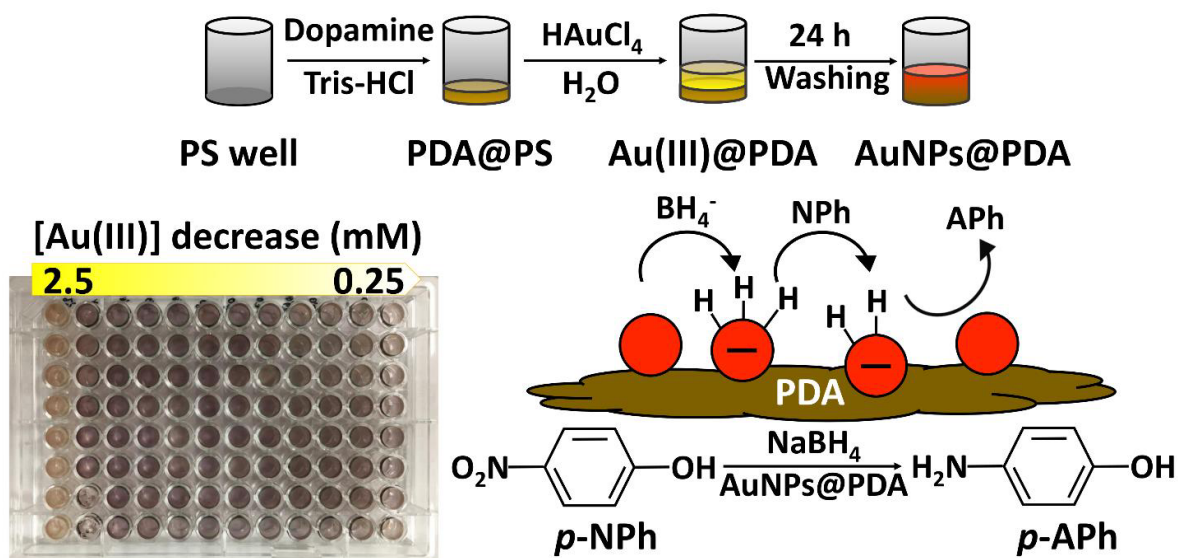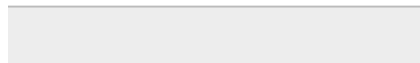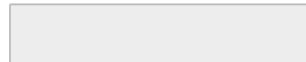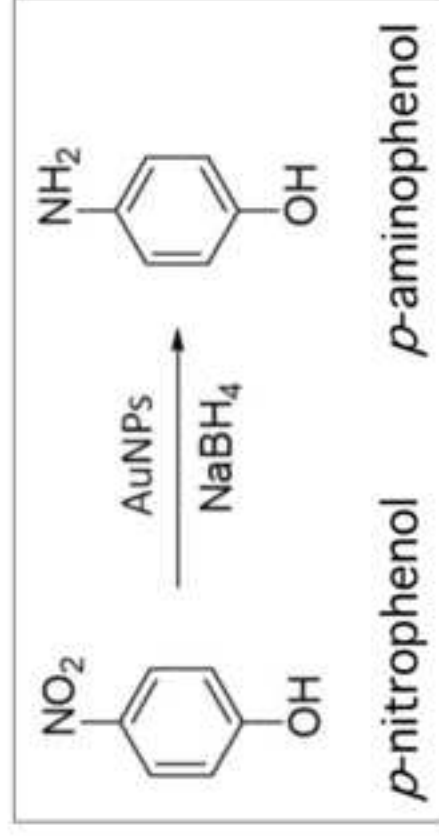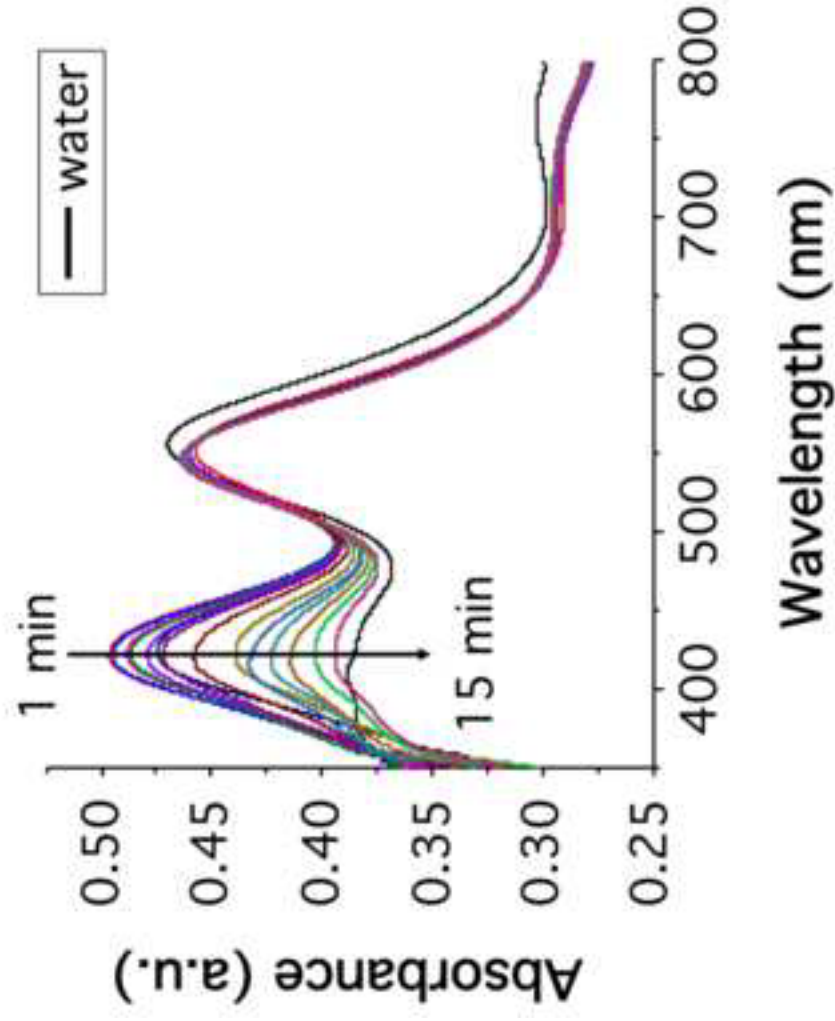
Schematic presentation of 96-wells preparation for optical quantification on ELISA reader of p-nitrophenol (p-NPh) catalytic reduction to p-aminophenol (p-APh), as model study, by $NaBH_4$ and different population gold nanoparticles (AuNPs) grown on polydopamine (PDA) films attached onto polystyrene (PS) wells.
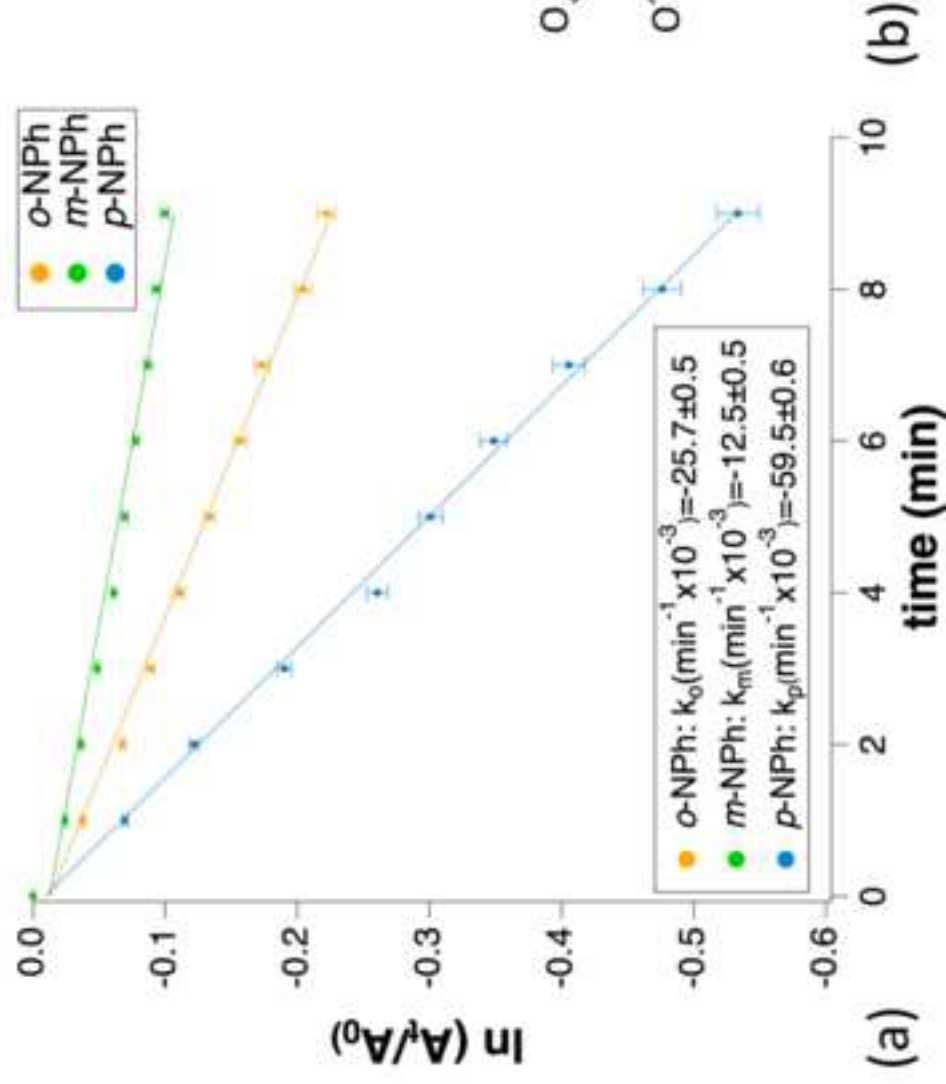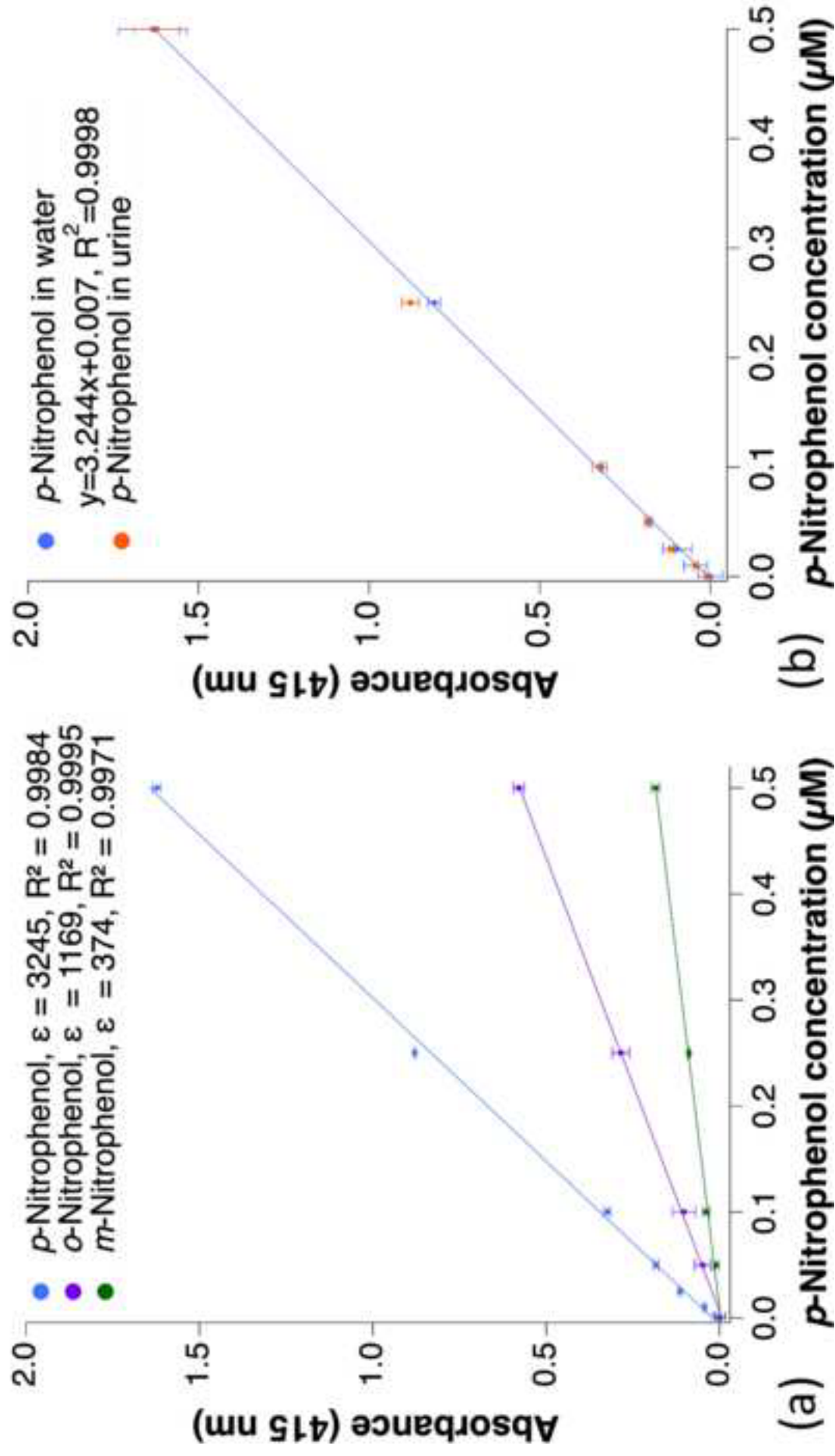
Click here to access/download
Electronic Supplementary Material
Electronic Supplementary Material (ESM)
14_01_2019.docx

Figure 1

Figure 2

(a)

(b)

Figure 3

(a) Absorbance (415 nm) vs. p-Nitrophenol concentration (µM)

p-Nitrophenol, ε = 3245, R² = 0.9984
o-Nitrophenol, ε = 1169, R² = 0.9995
m-Nitrophenol, ε = 374, R² = 0.9971

(b) Absorbance (415 nm) vs. p-Nitrophenol concentration (µM)

p-Nitrophenol in water
y=3.244x+0.007, R² =0.9998
p-Nitrophenol in urine

Table 1

Table 1
Recovery data at different concentrations of pNPh in urine samples. Standard deviations (SD) are calculated on n=5 independent replicates on the same microwell plate.

Spiked pNPh (μM)	Absorbance±SD in urine (a.u.)	Absorbance±SD in water (a.u.)	Recovery in urine (%)
0.500	1.623±0.066	1.634±0.100	99.3
0.250	0.879±0.025	0.809±0.019	108.6
0.100	0.325±0.022	0.320±0.005	101.5
0.050	0.184±0.007	0.177±0.006	103.6
0.025	0.114±0.008	0.097±0.042	118.3
0.010	0.043±0.007	0.043±0.034	100.0
0.000	0.010±0.008	0.010±0.036	100.0